A New Shearlet Hybrid Method for Image Denoising

E. Ehsaeyan*(C.A.)

Abstract: Traditional noise removal methods like Non-Local Means create spurious boundaries inside regular zones. Visushrink removes too many coefficients and yields recovered images that are overly smoothed. In Bayesshrink method, sharp features are preserved. However, PSNR (Peak Signal-to-Noise Ratio) is considerably low. BLS-GSM generates some discontinuous information during the course of denoising and destroys the flatness of homogenous area. Wavelets are not very effective in dealing with multidimensional signals containing distributed discontinuities such as edges. This paper develops an effective shearlet-based denoising method with a strong ability to localize distributed discontinuities to overcome this limitation. The approach introduced here presents two major contributions: (a) Shearlet Transform is designed to get more directional subbands which helps to capture the anisotropic information of the image; (b) coefficients are divided into low frequency and high frequency subband. Then, the low frequency band is refined by Wiener filter and the high-pass bands are denoised via NeighShrink model. Our framework outperforms the wavelet transform denoising by %7.34 in terms of PSNR (peak signal-to-noise ratio) and %13.42 in terms of SSIM (Structural Similarity Index) for 'Lena' image. Our results in standard images show the good performance of this algorithm, and prove that the algorithm proposed is robust to noise.

Keywords: Image Denoising, Shearlet Transform, NeighShrink, Wiener Filter, PSNR, SSIM, Wavelet, Edge Preserving, Threshold, SUREshrink.

1 Introduction

Restoring images contaminated by measurement errors that cause noise is an important problem in signal processing. Originally, shearlets have been introduced in 2006 as a new multiscale analysis tool [1] and developed by Ma [2-3]. This transform like curvelet and contourlet has good properties of multiscale, localization, anisotropy and directionality which can preserve edges efficiently. To date, a variety of applications of shearlet have been devised [4-6]. Gao has proposed an image denoising method in non-subsampled shearlet domain by introducing a multivariate shrinkage function for level thresholding [7]. A denoising algorithm for Synthetic Aperture Radar (SAR) images, has been suggested [8]. This algorithm utilizes shearlet transform to present multiscale resolutions and cycle spinning to suppress the Gibbs-like phenomena. Wang *et al.* have combined shearlet transform and hidden Markov tree model and introduced a novel image denoising method which can preserve edges efficiently [9].

Iranian Journal of Electrical & Electronic Engineering, 2016.
Paper received 20 February 2016 and accepted 30 April 2016.
* The Author is with the Department of Electrical Engineering, Sirjan University of Technology, Sirjan, Iran.
E-mail: ehsaeyan@sirjantech.ac.ir.

An edge and texture preserving denoising technique based on shearlet transform and Twin Support Vector Machines (TSVMs) has been reported [10]. A new form of shearlet system with low redundancy named Gabor shearlet, which can be implemented with standard wavelet filters and Gabor windows, has been applied [11]. In another research, non-subsample shearlet domain has been used for despeckling of ultrasound medical images [12]. In this method, adaptive anisotropic diffusion preserves edges and details, when applied to low frequency coefficients. An efficient two-stage shearlet-based impulse noise removal algorithm has been reported [13]. The authors used Highly Effective Impulse Noise Detection algorithm (HEIND) to find the location of noisy pixels and inpainting algorithm to reconstruct missed information and restore the image. A despeckling method based on nonlinear fusion technique and non-subsampled shearlet transform has been made for ultrasound images [14]. This method utilizes anisotropic diffusion to refine coarser shearlet coefficients while preserving the details.

Lie has considered non-subsampled shearlet transform and proposed a novel denoising scheme for natural images as well as infrared images [15]. He utilized shearlet transform to obtain the multiscale analysis and intuitionistic fuzzy entropy to refine noisy

pixels adaptively. A new denoising method for hyperspectral images based on shearlet transform has been carried out [16]. In this method, low levels of Gaussian noise and mixed noise bands are distinguished according to spectral coloration criterion, where a thresholding technique is used on low levels of Gaussian noise and local noise removal strategy is used on mixed noise bands.

In this paper, we propose an effective method for denoising images based on combining the shearlet transform with NeighShrink SURE (Stein's Unbiased Risk Estimator) and Wiener filter techniques. In our procedure, the image is decomposed into different subbands of coefficients with applying shearlet transform. Considering the difference between the low-and-high frequency sub-band coefficients, the low frequency sub-band coefficients are denoised by the Wiener filter and the high frequency sub-band coefficients are refined with a strategy based on NeighShrink SURE technique. At the end, with combination of low and high subbands, an inverse shearlet transform is applied and the restored image is obtained.

The organization of this paper is as follows: In Section 2, we give a brief overview of the shearlet transform and describe the basics of this transformation. After reviewing and discussing the preliminary theories, we present a new hybrid method which exploits the best features of shearlets and NeighShrink to obtain superior denoising capabilities in Section 3. In Section 4, we present the ability of the proposed method in denoising and discuss the experimental results of the comparison among different state-of-the-art techniques, and show that the method we have proposed, yields significantly better outcomes. The concluding remarks are given in Section 5.

2 Shearlet Transform

The shearlet transform is unlike the traditional wavelet transform which does not possess the ability to detect directionality, since it is merely associated with two parameters, the scaling parameter and the translation parameter. The idea is to define a transform, which overcomes this vice, while retaining most aspects of the mathematical framework of wavelets, e.g., the fact that:

- The associated system forms an affine system,
- The transform can be regarded as matrix coefficients of a unitary representation of a special group,
- There is an MRA[1]-structure associated with the systems.

The shearlets satisfy all these properties in addition to showing optimal behavior with respect to the detection of directional information. Shearlet transform is an example of composite wavelets, where $A = A_0 = \begin{bmatrix} 4 & 0 \\ 0 & 2 \end{bmatrix}$ and $B = B_0 = \begin{bmatrix} 1 & 1 \\ 0 & 1 \end{bmatrix}$ stand for anisotropic dilations matrix; and shear matrix, respectively. For any $\xi = (\xi_1, \xi_2) \in \hat{\mathcal{R}}^2$, $\xi_1 \neq 0$, $\psi^{(0)}$ satisfies [17]

$$\hat{\psi}^{(0)}(\xi) = \hat{\psi}^{(0)}(\xi_1, \xi_2) = \hat{\psi}_1(\xi_1)\hat{\psi}_2(\tfrac{\xi_2}{\xi_1}) \quad (1)$$

where $\hat{\psi}^{(0)}$ stands for Fourier transform of $\psi^{(0)}$, ψ_1 stands for continuous wavelet function, and $\hat{\psi}_1{}^{(0)} \in C^{\infty}(\mathcal{R})$, supp $\hat{\psi}_1 \subset \left[-\frac{1}{2}, -\frac{1}{16}\right] \cup \left[\frac{1}{16}, \frac{1}{2}\right]$, $\hat{\psi}_2$ stands for bump function and $\hat{\psi}_1 \in C^{\infty}(\mathcal{R})$, supp $\hat{\psi}_2 \subset [-1, -1]$. Therefore, $\hat{\psi}^{(0)}$ is a continuous and tight support, $\hat{\psi}^{(0)} \in C^{\infty}(\mathcal{R})$, supp $\hat{\psi}^{(0)} \in \left[-\frac{1}{2}, \frac{1}{2}\right]^2$. The induced tiling of the frequency plane is illustrated in Fig. 1(a). We suppose

$$\sum_{j\geq 0} \left|\hat{\psi}_1(2^{-2j}\omega)\right|^2 = 1, \quad |\omega| \geq \tfrac{1}{8} \quad (2)$$

and for $j \geq 0$

$$\sum_{l=-2^j}^{2^j-1} \left|\hat{\psi}_2(2^j\omega - l)\right|^2 = 1, \ |\omega| \leq 1 \quad (3)$$

By observing formulas (2) and (3), for any $(\xi_1, \xi_2) \in D_0 = \left\{(\xi_1, \xi_2) \in \mathcal{R}^2 : |\xi_1| \geq \frac{1}{8}, \left|\frac{\xi_2}{\xi_1}\right| \leq 1\right\}$, there exists:

$$\sum_{j\geq 0} \sum_{l=-2^j}^{2^j-1} \left|\hat{\psi}^{(0)}\left(\xi A_0^{-j} B_0^{-l}\right)\right|^2 =$$

$$\sum_{j\geq 0} \sum_{l=-2^j}^{2^j-1} \left|\hat{\psi}_1(2^{-2j}\xi_1)\right|^2 \left|\hat{\psi}_2(2^j \tfrac{\xi_2}{\xi_1} - l)\right|^2 = 1 \quad (4)$$

The fact that $\hat{\psi}_1$ and $\hat{\psi}_2$ are supported inside $2^{2j} \times 2^j$, (Fig. 1(b)), oriented along the straight line with slope $l2^{-j}$, implies that the collection of functions is defined by:

$$supp\ \hat{\psi}_{j,k,l}{}^{(0)} \subset \{(\xi_1, \xi_2)\} \quad (5)$$

where $\xi_1 \in [-2^{2j-1}, -2^{2j-4}] \cup [2^{2j-4}, 2^{2j-1}]$, $\left|\frac{\xi_2}{\xi_1} + l2^{-j}\right| \leq 2^{-j}$.

3 Proposed Scheme

The schematic of the proposed approach is illustrated in Fig. 2. The overall procedure of our proposed scheme can be summarized as follows:

Firstly, the Additive White Gaussian Noise is added to the standard image and the noisy image is decomposed in the shearlet domain and multi-scale and multi-directional sub images can be obtained in each band. Coefficients are divided into two groups, low and high frequencies. Unlike the low-frequency component, the high-frequency sub images place great emphasis upon the description of the information of edges and details in original source images. Hence, we separate them in the denoising process. Instead of the method introduced in [14], which keeps low frequency coefficients unchanged, we apply adapting Wiener filter [18] to the lowpass subband and NeighShrink algorithm to the high frequency algorithm. Wiener filter is selected in lowpass coefficients, because it is optimal in minimizing the mean squared estimation error and

[1] Multiresolution Analysis

NeighShrink is considered in highpass frequency bands, due to its advantage to yield good smoothing images.

Finally, by using the inverse shearlet transform, the final denoised image can be obtained.

NeighShrink denoising algorithm is as follows [19]:

Step 1: Divide coefficients at level j to disjoint blocks $U_{i,j}$ with size 3×3 and 5×5;

Step 2: Shrink the wavelet coefficients $d_{i,j}$ by using the following formula, denoting the new coefficients by $\hat{d}_{i,j}$,

$$\hat{d}_{i,j} = d_{i,j}\beta_{i,j} \quad (6)$$

where $\beta_{i,j}$ is the shrinkage factor that is given as follows:

$$\beta_{i,j} = \left(1 - \frac{T^2}{S_{i,j}^2}\right)_+ \quad (7)$$

in which $S_{i,j}^2 = \sum_{(p,q)\in U_{i,j}} d_{p,q}^2$. Here, "+" sign at the end of the formula means to keep the positive values, and negative values are set as zero. This denoising model can be used for each shearlets scale.

4 Results and Discussions

In this section, simulations are carried out using standard images to investigate the performance of the proposed method. The AWGN noise is applied to standard images to provide noisy input images. In our method, the decomposition level of the shearlet transform is set to 4, the numbers of shearing directions are chosen to be 4, 4, 4 and 4 from finer to coarser.

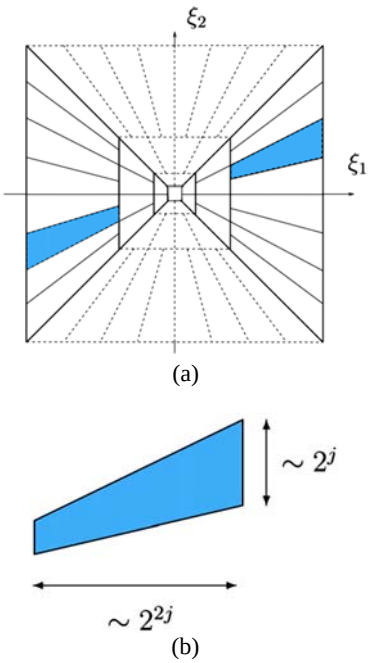

Fig. 1 Spatial-frequency plane and frequency support of shearlets. The illustrations have been taken from [17]. (a) The tiling of the special-frequency plane induced by the shearlets (b) The frequency support of shearlets.

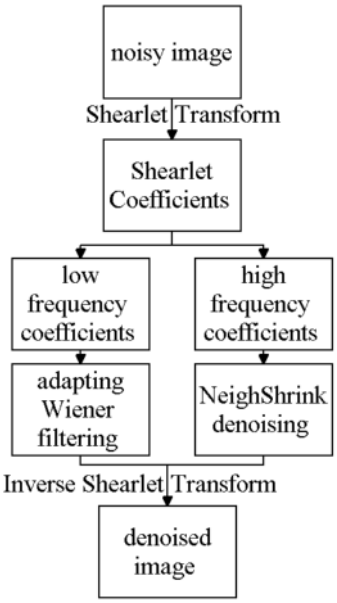

Fig. 2 The architecture of the proposed denoising method.

If the decomposition level of the shearlet transform is low, noise could not be removed efficiently. However, the denoised image would be similar to the main image. If the decomposition level is high, the output would be a filtered image. However, some artifact would be added to it. Also, the computational cost would be increased. Figure 3 shows these manner for image 'cameraman' in $sigma = 30$.

Another parameter which affects the denoised image, is the number of shearing directions. In low directions, the denoised image has artifacts and in high directions, the line-shaped spurs are suppressed. However, the image would be blurred. Figure 4 illustrates this effect.

The size of the window in adapting Wiener filter is set to 7×7. We found that in our proposed algorithm, the windows size 3×3 approximately satisfies the best condition and the use of window size 5×5 instead of 3×3 yields a slightly better performance. With these conditions, threshold levels are calculated for each scale. We use SURE shrink to estimate the noise level of every directional band and apply hard threshold to its coefficients. There is a slight difference between our threshold levels and optimal ones. Table 1 shows these differences for the image 'Cameraman' in various noisy conditions. The optimal thresholds have been obtained by numerical solution to reach maximum PSNRs.

A comparison between our threshold levels and optimum ones in PSNRs, is presented in Figure 5. Error bars show the deviation of optimum PSNRs. According to this figure, we found that the difference between the output of our thresholds and optimal ones becomes larger with the increase of noise level.

(a) Noisy image PSNR=18.61 dB

(b) level=2 PSNR=24.82 dB

(c) level=4 PSNR=26.8 dB

(d) level=6 PSNR= 27.26 dB

Fig. 3 The effect of increasing decomposition level on output image.

(a) Noisy image PSNR=18.61 dB

(b) 2 directions PSNR=27.00 dB

(c) 4 directions PSNR=27.19 dB

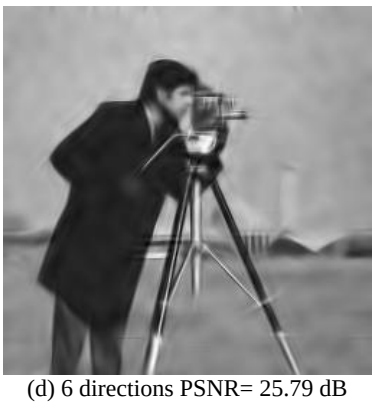

(d) 6 directions PSNR= 25.79 dB

Fig. 4 The effect of increasing directional level on output image.

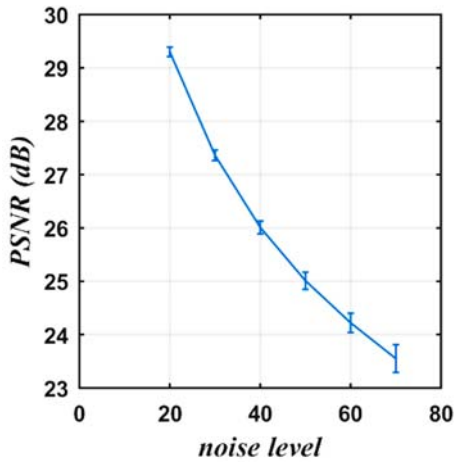

Fig. 5 The difference between our obtained thresholds and optimal thresholds (Table 1) in term of PSNR.

Table 1 Threshold results of our method against optimal ones for image 'Cameraman'.

	Threshold Levels	
Sigma	Ours	Optimum
20	3.057	2.60
	2.99	2.60
	2.78	2.50
	2.76	3.00
30	2.79	2.60
	2.73	2.60
	2.92	2.5
	2.92	3.1
40	2.57	2.60
	2.50	2.60
	2.98	2.5
	2.98	3.1
50	2.53	2.60
	2.42	2.60
	3.17	2.5
	3.14	3.4
60	2.37	2.60
	2.24	2.60
	3.19	2.6
	3.19	3.4
70	2.14	2.60
	2.05	2.60
	3.08	2.7
	3.08	3.6

We compare the results of our approach with some other famous methods including ProbShrink[1] [20], BLS-GSM[2] [21], SUREbivariate[3] [22], NL-means[4] [23] and TV[5] model [24] with standard images database [25]. Denoising results for different algorithms are shown in Figure 6. It is clear that the introduced algorithm consistently outperforms all the algorithms mentioned above. The improvement is in many cases, 1 dB or more.

In order to evaluate the performance of the proposed technique in preserving edge information, simulation experiments of shearlet denoising and wavelet denoising have been carried out on the 'Peppers' image. Additive Gaussian white noises with different standard deviations have been added and the results are shown in Fig. 7.

Simulations carried out on the Peppers image demonstrate that the visual quality of the shearlet results is more excellent in terms of both background smoothing and preservation of edge sharpness and textures especially in high noise level. Furthermore, we compare our proposed against well-known methods in terms of SSIM [26]. Results are shown in Table 2. The size of images is 512×512.

Table 2 SSIM Comparison of the performances of the proposed algorithm to other algorithms (These results were published in [27] and were directly imported from that).

Sigma	**10**	**20**	**30**
Lena 512×512			
Linear Local SURE method	0.89	0.84	0.78
Guided Image Filter method	0.88	0.81	0.76
Fast Bilateral Filter method	0.88	0.82	0.74
TV method	0.87	0.83	0.77
SURELET method	**0.90**	0.84	0.8
Besov method	0.85	0.78	0.73
Bays method	0.87	0.8	0.76
LAPB [27]	**0.90**	0.84	0.81
our method	**0.90**	**0.86**	**0.82**
Barbara 512×512			
Linear Local SURE method	**0.91**	0.81	0.74
Guided Image Filter method	0.89	0.8	0.76
Fast Bilateral Filter method	0.9	0.8	0.74
TV method	0.9	0.81	0.75
SURELET method	0.9	0.8	0.71
Besov method	0.87	0.76	0.67
Bays method	0.85	0.74	0.67
LAPB [27]	**0.91**	0.84	0.77
Our method	**0.91**	**0.85**	**0.79**

[1] Probability Shrinkage

[2] Bayes Least Square Gaussian Scale Mixture

[3] Stein's Unbiased Risk Estimator Bivariate Shrinkage

[4] Non-Local Means

[5] Total Variation model

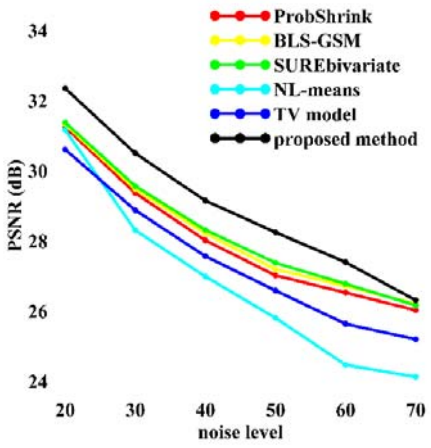

(a) Lena 512×512

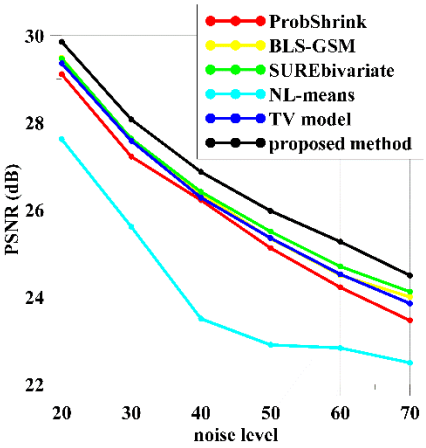

(d) Boat 512×512

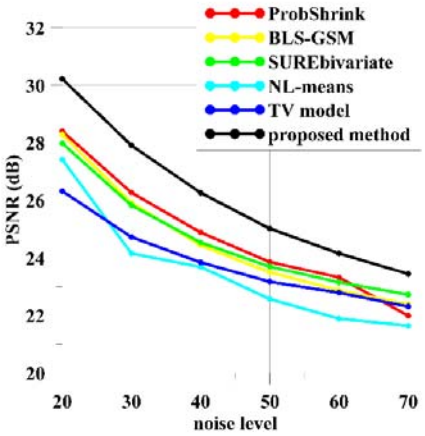

(b) Barbara 512×512

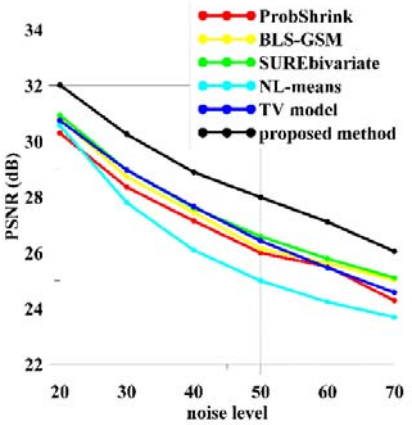

(e) House 256×256

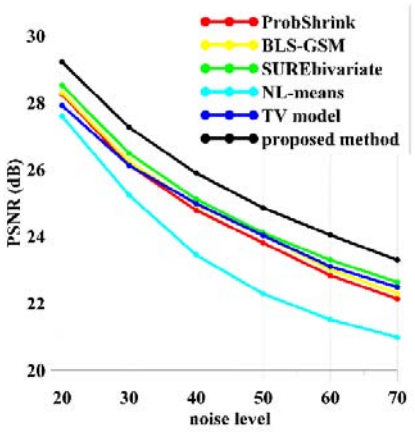

(c) Cameraman 256×256

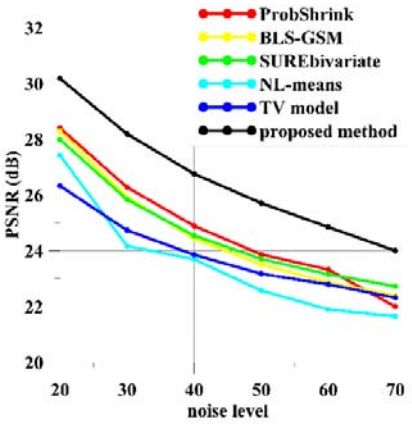

(f) Peppers 256×256

Fig. 6 The denoising results of different well-known methods for test images in term of PSNR

From Table 2, we can see that SSIMs of our approach are optimal compared to other algorithms. Finally, we included a comparison with recent reported denoising algorithm.The performance of our approach relative to other state-of-art methods is shown in Table 3.

The comparison of these results for standard images, indicates that the noise suppression ability of our method is the best in most cases.

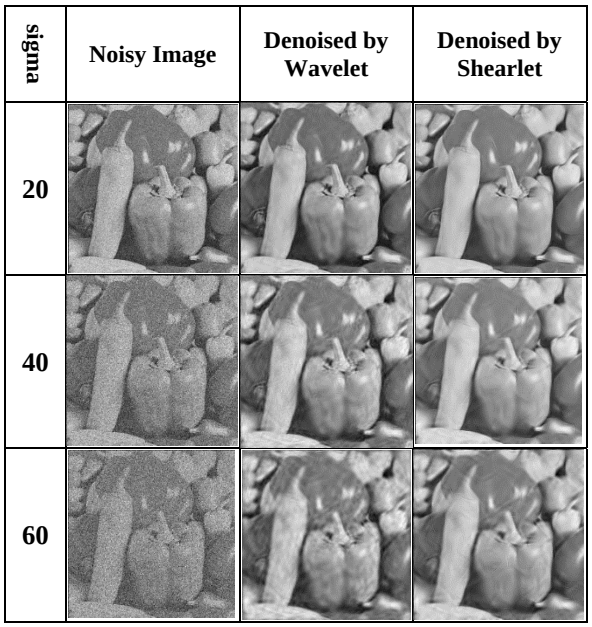

Fig. 7 The example of visual effects and quality evaluation. Denoised Peppers in different noise conditions.

Table 3 The comparison of denoised results in terms of PSNR (dB).

	Lena		Barbara		Peppers	
σ	20	30	20	30	20	30
[27]	31.74	29.71	29.16	27.51	30.75	29.02
[28]	30.77	29.04	28.55	27.38	30.57	28.83
[29]	30.92	29.13	28.48	26.27	30.57	28.83
[30]	28.25	25.7	26.81	24.49	26.96	25.03
[31]	31.16	29.25	28.71	26.59	30.81	28.92
[32]	30.61	28.73	26.57	26.36	29.31	27.85
[33]	30.42	28.54	26.28	24.73	30.17	28.28
[34]	31.71	29.82	29.86	**27.94**	30.01	28.14
Our Work	**32.35**	**30.49**	**30.22**	27.91	**31.75**	**30.18**

5 Conclusion

This paper presented a new approach for image denoising based on shearlet transform, Wiener filter and NeighShrink SURE model. In this method, to make the best result, the low frequency sub-band coefficients were denoised by applying the adaptive Wiener filter. As for the high frequency sub-band coefficients, they were refined according to the NeighShrink rule. In order to evaluate the performance of the proposed algorithm, experiments were performed on different standard images. The visual effect image and detailed measurements showed that our method is more effective, which is not only better in reducing noise, but also has an advantage in preserving the information of edges. Measured results revealed that our scheme had the best PSNRs in most cases. In future research, we intend to study how this hybrid method could be suitable for solving problems related to inpainting.

References

[1] K. Guo, G. Kutyniok, and D. Labate. "Sparse multidimensional representations using anisotropic dilation and shear operators," *Wavelets and Splines, Athens, GA*, vol. 1, pp. 189-201, 2005.

[2] J. Ma and P. Petersen, "Linear independence of compactly supported separable shearlet systems," *Journal of Mathematical Analysis and Applications*, vol. 428, no. 1, pp. 238–257, 2015.

[3] J. Ma, "Generalized sampling reconstruction from Fourier measurements using compactly supported shearlets," *Applied and Computational Harmonic Analysis, in Press*, DOI: 10.1016/j.acha.2015.07.006, 2015.

[4] H. Lakshman, W.-Q. Lim, H. Schwarz, D. Marpe, G. Kutyniok, and T. Wiegand, "Image interpolation using shearlet based iterative refinement," *Signal Processing: Image Communication*, vol. 36, pp. 83–94, 2015.

[5] S. Singh, D. Gupta, R. Anand, and V. Kumar, "Nonsubsampled shearlet based CT and MR medical image fusion using biologically inspired spiking neural network," *Biomedical Signal Processing and Control*, vol. 18, pp. 91-101, 2015.

[6] A.-U. Moonon and J. Hu, "Multi-Focus Image Fusion Based on NSCT and NSST," *Sens Imaging Sensing and Imaging*, vol. 16, no.1, pp. 1-16, 2015.

[7] G. Gao, "Image denoising by non-subsampled shearlet domain multivariate model and its method noise thresholding," *Optik-International Journal for Light and Electron Optics*, vol. 124, no. 22, pp. 5756–5760, 2013.

[8] S. Liu, M. Shi, S. Hu, and Y. Xiao, "Synthetic aperture radar image de-noising based on Shearlet transform using the context-based model," *Physical Communication*, vol. 13, no. C, pp. 221-229, 2014.

[9] X.-Y. Wang, Y.-C. Liu, and H.-Y. Yang, "Image denoising in extended Shearlet domain using hidden Markov tree models," *Digital Signal Processing*, vol. 30, pp. 101–113, 2014.

[10] H.-Y. Yang, X.-Y. Wang, P.-P. Niu, and Y.-C. Liu, "Image denoising using nonsubsampled shearlet transform and twin support vector machines," *Neural Networks*, vol. 57, pp. 152-165, 2014.

[11] B. G. Bodmann, G. Kutyniok, and X. Zhuang, "Gabor shearlets," *Applied and Computational Harmonic Analysis*, vol. 38, no. 1, pp. 87–114, 2015.

[12] D. Gupta, R. Anand, and B. Tyagi, "Despeckling of ultrasound medical images using nonlinear adaptive anisotropic diffusion in nonsubsampled shearlet domain," *Biomedical Signal Processing and Control*, vol. 14, pp. 55–65, 2014.

[13] G. Gao, Y. Liu, and D. Labate, "A two-stage shearlet-based approach for the removal of random-valued impulse noise in images," *Journal of Visual Communication and Image Representation*, vol. 32, pp. 83–94, 2015.
[14] D. Gupta, B. Tyagi, and R. S. Anand, "Speckle filtering of ultrasound images using a modified non-linear diffusion model in non-subsampled shearlet domain," *IET Image Processing*, vol. 9, no. 2, pp. 107–117, 2015.
[15] Y. Lei, "Technique for image de-noising based on non-subsampled shearlet transform and improved intuitionistic fuzzy entropy," *Optik-International Journal for Light and Electron Optics*, vol. 126, no. 4, pp. 446–453, 2015.
[16] A. Karami, R. Heylen, and P. Scheunders, "Band-Specific Shearlet-Based Hyperspectral Image Noise Reduction," *IEEE Trans. Geosci. Remote Sensing IEEE Transactions on Geoscience and Remote Sensing*, vol. 53, no. 9, pp. 5054–5066, 2015.
[17] G. Easley, D. Labate, and W.-Q. Lim, "Sparse directional image representations using the discrete shearlet transform," *Applied and Computational Harmonic Analysis*, vol. 25, no. 1, pp. 25–46, 2008.
[18] J. S. Lim, *Two-dimensional signal and image processing*. Englewood Cliffs, N.J.: Prentice Hall, 1990, p. 548.
[19] T. Cai and B. W. Silverman, "Incorporating information on neighboring coefficients into wavelet estimation," *Sankhya, Ser*, vol. 63, pp. 127–148, 2001.
[20] A. Pizurica and W. Philips, "Estimating the probability of the presence of a signal of interest in multiresolution single- and multiband image denoising," *IEEE Transactions on Image Processing IEEE Trans. on Image Process.*, vol. 15, no. 3, pp. 654–665, 2006.
[21] J. Portilla, V. Strela, M. Wainwright, and E. Simoncelli, "Image denoising using scale mixtures of gaussians in the wavelet domain," *IEEE Transactions on Image Processing IEEE Trans. on Image Process.*, vol. 12, no. 11, pp. 1338–1351, 2003.
[22] F. Luisier, T. Blu, and M. Unser, "A New SURE Approach to Image Denoising: Interscale Orthonormal Wavelet Thresholding," *IEEE Transactions on Image Processing IEEE Trans. on Image Process.*, vol. 16, no. 3, pp. 593–606, 2007.
[23] A. Buades, B. Coll, and J. M. Morel, "A Review of Image Denoising Algorithms, with a New One," *Multiscale Modeling & Simulation Multiscale Model. Simul.*, vol. 4, no. 2, pp. 490-530, 2005.
[24] L. Rudin, S. Osher, and E. Fatemi, "Nonlinear total variation based noise removal algorithm," *Phys. D*, vol. 60, pp. 259–268, 1992.
[25] http://www.io.csic.es/PagsPers/JPortilla/image-processing/bls-gsm/63-test-images.
[26] Z. Wang, A. Bovik, H. Sheikh, and E. Simoncelli, "Image Quality Assessment: From Error Visibility to Structural Similarity," *IEEE Transactions on Image Processing IEEE Trans. on Image Process.*, vol. 13, no. 4, pp. 600–612, 2004.
[27] P. Jain and V. Tyagi, "LAPB: Locally adaptive patch-based wavelet domain edge-preserving image denoising," *Information Sciences*, vol. 294, pp. 164–181, February 2015.
[28] H. Om and M. Biswas, "A generalized image denoising method using neighbouring wavelet coefficients," *Signal, Image and Video Processing SIViP*, vol. 9, no. 1, pp. 191–200, 2013.
[29] H. Om and M. Biswas, "MMSE based map estimation for image denoising," *Optics & Laser Technology*, vol. 57, pp. 252–264, April 2014.
[30] P. Jain and V. Tyagi, "An adaptive edge-preserving image denoising technique using tetrolet transforms," *The Visual Computer Vis Comput*, pp. 657–674, 2014.
[31] M. Biswas and H. Om, "A New Adaptive Image Denoising Method Based on Neighboring Coefficients," *Journal of The Institution of Engineers (India): Series B J. Inst. Eng. India Ser. B*, 2014.
[32] D. Tian, D. Xue, and D. Wang, "A fractional-order adaptive regularization primal–dual algorithm for image denoising," *Information Sciences*, vol. 296, pp. 147–159, March 2015.
[33] N. He, J.-B. Wang, L.-L. Zhang, and K. Lu, "An improved fractional-order differentiation model for image denoising," *Signal Processing*, vol. 112, pp. 180–188, July 2015.
[34] F. Chen, X. Zeng, and M. Wang, "Image denoising via local and nonlocal circulant similarity," *Journal of Visual Communication and Image Representation*, vol. 30, pp. 117–124, July 2015.

Ehsan Ehsaeyan received the B.Sc. degree in electronic engineering from Shahed University, Tehran, Iran in 2006 and the M.Sc. Eng degree in communication engineering at University of Shahid Bahonar, Kerman, Iran in 2009. His research interest is image processing and RF communication.